Journal of the European Ceramic Society 22 (2002) 159–164

www.elsevier.com/locate/jeurceramsoc

Effect of glass additives on the strength and toughness of polycrystalline alumina

Yi-Quan Wu [a,*], Yu-Feng Zhang [a], Giuseppe Pezzotti [b], Jing-Kun Guo [a]

[a] *State Key Lab of High Performance Ceramics and Superfine Microstructure, Shanghai Institute of ceramics, Chinese Academy of Sciences, Shanghai 200050, China*

[b] *Department of Materials, Kyoto Institute of Technology, Sakyo-ku, Matsugasaki, Kyoto-shi 606, Japan*

Received 23 September 2000; received in revised form 15 February 2001; accepted 23 February 2001

Abstract

The effect of stress at grain boundaries on the mechanical properties of alumina ceramics was investigated. Residual stresses at grain-boundaries resulted from a mismatch in thermal expansion coefficient (TEC) between the alumina matrix and the glass-phase segregated at grain-boundaries. The $BaO–Al_2O_3–SiO_2$ (BAS) system and the $Li_2O–Al_2O_3–SiO_2$ (LAS) system glasses were chosen to have a higher and a lower TEC than that of alumina, respectively, resulting in microscopic tensile and compressive stresses at grain-boundaries for Al_2O_3/BAS and Al_2O_3/LAS composites, respectively. The experimental results showed that the Al_2O_3/BAS composite fractured intergranularly with a fracture toughness higher than that of monolithic alumina. On the other hand, the Al_2O_3/LAS composite experienced transgranular fracture and high bending strength despite its low toughness. Both composites could be sintered to full density at 1500°C for 2 h due to the presence of a liquid phase. It was concluded that strengthening and toughening of alumina ceramics could be tailored by designing their grain-boundary microstresses.

Keywords: Al_2O_3; Glass; Grain boundaries; Mechanical properties; Thermal expansion coefficient

1. Introduction

Most of ceramics are polycrystalline materials composed of grains and grain-boundaries whose physical and chemical characteristics can largely affect the structures properties of ceramics.[1–4] Practically, the important role of grain-boundaries has been widely recognized in designing and processing ceramics with high performance. For example, the concept of ''grain-boundary engineering'' makes a great contribution to the design of ceramics with improved structures properties, such as Si_3N_4 and SiAlON ceramics.[5–10] It is also well known that grain-boundary chemistry can exert a significant effect on the mechanical properties of ceramics, such as strength, fracture toughness, creep and superplasticity.[11–18] As widely recognized in recent studies[19,20], if there is a difference in the shrinkage rate between grains and grain-boundary phase, residual stresses are induced at grain-boundaries during the cooling of the ceramics from sintering temperature. By a liquid-phase sintering process, ceramics can be sintered with different liquid-forming additives which lower the sintering temperature, thus forming thin continuous or semicontinuous glass phases at grain boundaries. At room temperature, residual stress results from the mismatch in thermal expansion coefficient (TEC) of the grain-boundary glass and the crystalline matrix.[21,22] Residual microstress at grain-boundaries has a significant effect on the crack propagation mode and thus on the mechanical properties of polycrystalline ceramics.[23–26] Generally, when the TEC of the grain-boundary phase is greater than that of grains, a tensile stress field will be generated at grain-boundaries. While, for equilibrium to be kept, compressive stress will be generated in the grains. The tensile stress at the grain boundary is expected to drive the crack path along the intergranular glass phase, resulting in intergranular fracture mode. This may in turn lead to a higher fracture toughness. When the TEC of the grain-boundary phase is lower than that of the crystalline grains, there will be compressive stress at grain

* Corresponding author.
E-mail address: yiquanwu@netease.com (Y.-Q. Wu).

0955-2219/01/$ - see front matter
PII: S0955-2219(01)00253-9

boundaries, resulting in a transgranular fracture mode. Despite a low fracture toughness, these materials may show a high bending strength.[27–30] With this understanding, we can design residual stresses at ceramic grain-boundaries to achieve the desired mechanical properties.

In this paper, we studied the effect of grain-boundary stresses on the bending strength and fracture toughness of alumina ceramics with added $BaO–Al_2O_3–SiO_2$ (BAS) and Li_2O-Al_2O_3-SiO_2 (LAS) glass-phases, whose TECs were chosen to be higher and lower than that of alumina grains, respectively. The barium aluminosilicate system is ideal for designing higher thermal expansion glass phases, because upon crystallization taking place during cooling, the high temperature form of the crystalline phase, $BaAl_2Si_2O_8$ shows higher TEC than that of alumina. On the other hand, in the tri-element phase-diagram of the $Li_2O–Al_2O_3–SiO_2$ system, there is a zone of lower TEC as compared to alumina. The present study discusses the possibility of controlling grain-boundary stresses in order to confer desirable properties on alumina ceramics.

2. Experimental procedures

The LAS and BAS glasses were prepared by milling mixtures of 22.9 wt.% Al_2O_3, 60.4 wt.% SiO_2 with 16.7 wt.% Li_2CO_3, and 18.3 wt.% Al_2O_3, 24.9 wt.% SiO_2 with 56.8 wt.% $BaCO_3$, respectively. Then, melting at 1550°C for 6 h and quenching in cold distilled water were performed. The transparent glasses were crushed to <1 mm and milled with high-purity alumina mediums. High-purity commercial alumina powder was, respectively, mixed with 5 wt.% BAS and 5 wt.% LAS glass powders in ethanol for 24 h using high-purity alumina balls. After drying, sieving through 120 μm net, PVA was added. The mixed powders were uniaxially pressed at 100 MPa and then cold isostatically pressed at 250 MPa. The green samples were packed in loose alumina powder inside an alumina crucible and calcined at 700°C for 1 h, followed by sintering at 1500°C for 2 h. For comparison, monolithic alumina was also prepared by the same sintering schedule.

The bending strength was measured in three-point bending with a span of 20 mm and a crossed speed at 0.5 mm/min at room temperature using an Instron 1195 Universal Test Machine. The tensile surface of the bend bars was polished and the edge chamfered to mirror surface. The dimension of test pieces was $2.5\times5\times25$ mm. Fracture toughness, K_{IC}, was determined using an indentation technique with a Vicker Indenter (AKASHI) using 98N load. The equation used for calculating K_{IC} was that proposed by Anstis et al.[31] A number of specimens $\geqslant6$ was tested for each data point. The thermal expansion coefficient of the bulk glasses was measured using an alumina rod dilatometer (Netzsch-402ES, Germany).

The presence of crystalline phases of sintered bulk samples was identified by X-ray diffraction (XRD) (D/max-radiffractometer, Rigaku,Japan) analysis with Ni filtered CuK_α radiation. The samples for microstructural observation were cut from the sintered bodies, polished and chemically etched in 0.1 N HF acid at 50°C for 8–10 s. Both etched surfaces and fracture surfaces were observed with a scanning electron microscope (SEM) (EPMA-8705QHz, Shimadzu, Japan). A transmission electron microscope (TEM) (JEM-200cx, JEM-400cx, Jeol, Japan) equipped with X-ray energy dispersive spectroscopy (EDS) was used to obtain the chemical composition of the grain boundary phases. TEM specimens were prepared following the standard procedure of cutting, polishing and Ar-ion-milling to perforation. TEM specimens were coated with a thin layer of evaporated carbon to suppress charging.

3. Results and discussion

3.1. Microstructural characterizations

The X-ray diffraction patterns of the sintered samples are shown in Fig. 1. It can be seen from the figure that the only crystalline phase in the Al_2O_3/5 wt.% LAS composite is α-Al_2O_3 phase, while the crystalline phases

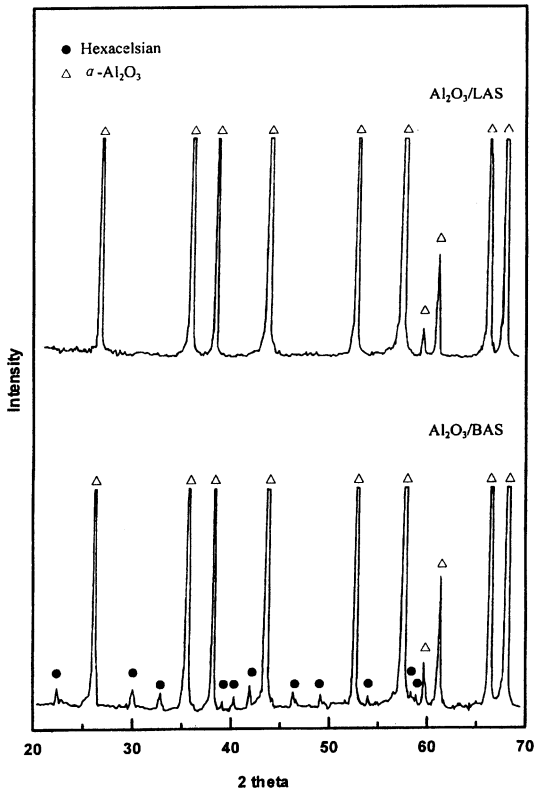

Fig. 1. XRD pattern of Al_2O_3/5 wt.% LAS and Al_2O_3/5 wt.% BAS composites sintered at 1500°C for 2 h.

in the Al_2O_3/5 wt.% BAS composite are α-Al_2O_3 phase and a minor fraction of hexacelsian phase. This indicates that LAS glass in the composite did not crystallize during cooling, while BAS glass showed a slight crystallization. The different crystallization behavior is thought to be due to both differences in glass composition and crystallization kinetics.

SEM micrographs of polished surfaces are shown in Fig. 2(a) and (b) for the Al_2O_3/5 wt.% LAS and Al_2O_3/5 wt.% BAS, respectively. The microstructure in Fig. 2(a) shows both equaxied and platelet α-Al_2O_3 grains of a similar size. When etching, the glass phase at grain boundaries and triple-grains junctions was leached out. The resulting Al_2O_3 skeleton suggests that alumina and glass were interpenetrating phases. For Al_2O_3/LAS composite, a TEM analysis revealed no crystalline phases, as shown in Fig. 3, the selected-area diffraction (SAD) patterns at triple-grain junctions systematically showing a halo pattern, inset in Fig. 3. A combined analysis of TEM and EDS indicated that the glass-phase at triple-grain junctions possessed an average composition of 15.2±0.2 mol% Li_2O, 16.0±0.3 mol% Al_2O_3 and 68.8±0.2 mol% SiO_2. Fig. 2(b) for the Al_2O_3/BAS composite shows almost equaxied α-Al_2O_3 grains with a minor fraction small crystallines precipitated from the liquid-phase at triple-grain junctions, the glass residue being etched out. The LAS system reveals some extended Al_2O_3 regions and the BAS system shows continuous grain-boundary wetting, this difference was due to the different etching ratio and grain-boundary width for LAS and BAS glasses. The differences in wetting behavior and glass phase/ Al_2O_3 distribution also may have some effects. A TEM image of the Al_2O_3/BAS composite is shown in Fig. 4 that reveals the presence of both residual glass-phase and crystalline phase. The SAD pattern collected at the location A inset in Fig. 4 confirms the presence of amorphous phase. Quantitative EDS analyses of the precipitated crystalline phase at triple-grain junctions (region A in Fig. 5) yielded an average composition of 32.8±0.5 mol% BaO, 19.8±0.2 mol% Al_2O_3 and 47.4±0.4 mol% SiO_2, which is not far from the stoichiometric composition of $BaAl_2Si_2O_8$, the EDS is shown in Fig. 6. Chemical identification of the hexacelsian phase was confirmed by electron diffraction pattern, shown in Fig. 5. Having both the investigated ceramics a similar grain size, it is originated that composition and viscosity

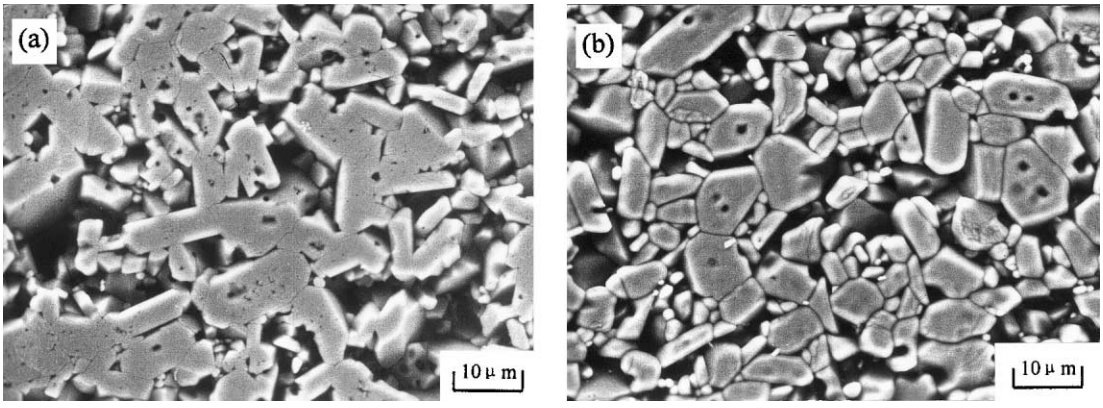

Fig. 2. SEM micrographs of composite etched surfaces: (a) Al_2O_3/5 wt.% LAS; (b) Al_2O_3/5 wt.% BAS.

Fig. 3. TEM microstructural characteristics of Al_2O_3/5 wt.% LAS composite with an EDS pattern of grain boundaries.

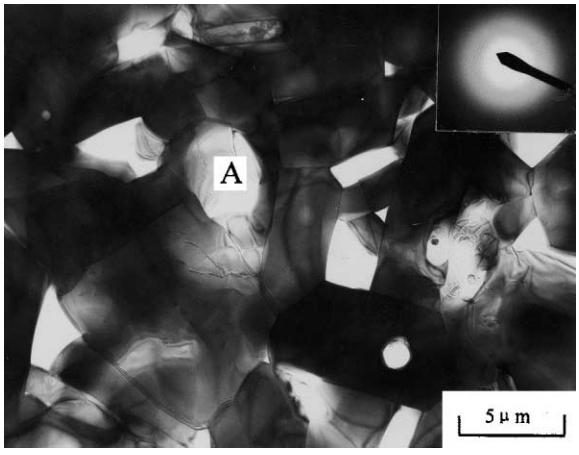

Fig. 4. TEM microstructural characteristics of Al_2O_3/5 wt.% BAS composite with an EDS pattern of point A.

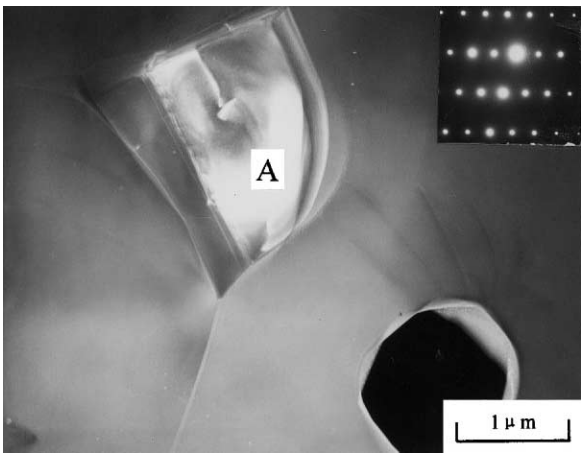

Fig. 5. TEM micrograph of three-grain boundary of Al_2O_3/5 wt.% BAS composite with an EDS pattern point of A.

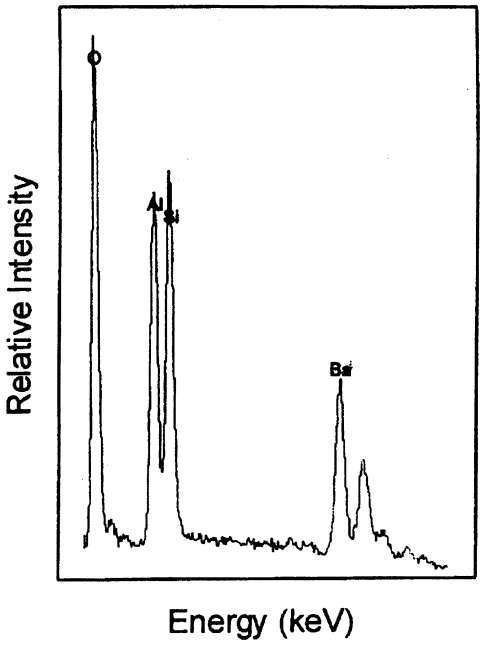

Fig. 6. An EDX spectrum obtained from the region shown in point A in Fig. 6.

of LAS and BAS glasses have no significant influence on the microstructure for Al_2O_3-based composites. SEM micrographs of fracture surfaces of the composites are shown in Fig. 7. The fracture mode for Al_2O_3/LAS and Al_2O_3/BAS composites was almost completely transgranular and intergranular, respectively.

3.2. Residual stresses and mechanical properties

Table 1 lists the TEC of intergranular glasses and the mechanical properties of Al_2O_3/5 wt.% LAS and Al_2O_3/5 wt.% BAS composites in comparison with monolith Al_2O_3. It can be seen from the table that the Al_2O_3/LAS composite experience higher bending strength and lower fracture toughness than monolithic Al_2O_3 ceramics, while the opposite trend is found for Al_2O_3/BAS. This can be attributed to the different residual stresses at grain-boundaries, resulting from the difference in TEC between alumina grains and the glass-phase. Since the precise composition of the glass is known, it is possible to estimate the TEC value of the glass from standard data using a linear equation.[32] The LAS glass-phase in this study had TEC of 4.36×10^{-6} K^{-1}, lower than that of Al_2O_3 ($6–8\times10^{-6}$ K^{-1}), thus compressive stress formed at grain boundaries inhibiting the crack to propagate in intergranular fashion. Stress fringes resulting from stress created by thermal expansion mismatch could be observed by TEM in the alumina grain, as shown by arrow in Fig. 3. The BAS glass and the crystalline hexacelsian phase ($\alpha \geqslant 8.0\times10^{-7}/^{\circ}C$)[33] had higher TEC than Al_2O_3, the TEC of BAS glass also increasing upon crystallization, so the residual stresses developed at grain boundaries is expected to be of tensile stress. Microcracks resulted from such tensile stresses that can be seen in Fig. 5 (shown by arrow), as a result of the higher thermal expansion of both hexacelsian phase and BAS glass-phase trapped within the alumina grains (point B). Grain-boundary microcracking, generated by grain-boundary tensile microstresses, triggers intergranular fracture and results in a higher fracture toughness, but a lower bending strength.

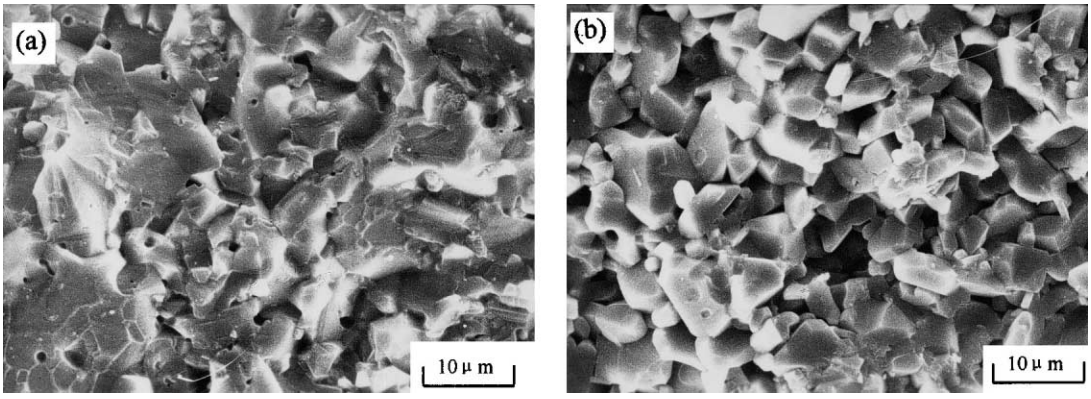

Fig. 7. SEM micrographs of composite fracture surfaces: (a) Al_2O_3/5 wt.% LAS; (b) Al_2O_3/5 wt.% BAS.

Table 1
The composition and TEC of the glass and the mechanical properties of the composites

Composites	Glass compostion (wt.%)				α (10^{-6}/°C)	Bending strength (MPa)	Fracture toughness (MPa $m^{1/2}$)
	Al_2O_3	SiO_2	Li_2O	BaO			
Al_2O_3/5 wt.% LAS	25.4	67.1	7.5	–	4.36	404±30	3.44±0.2
Al_2O_3/5 wt.% BAS	21.0	28.5	–	50.5	10.7	273±42	4.76±0.3
Al_2O_3	–	–	–	–	6–8	336±28	3.80±0.2

4. Conclusion

1. Al_2O_3/5 wt.% BAS composite sintered at 1500°C for 2 h showed intergranular fracture mode with an average fracture toughness of 4.76±0.3 MPa·$m^{1/2}$ and bending strength 273±42 MPa because the BAS glass have higher TEC than alumina, resulting in tensile microstresses at grain boundaries.
2. Al_2O_3/5 wt.% LAS composite sintered at 1500°C for 2 h showed transgranular fracture mode with an average fracture toughness of 3.44±0.2 MPa $m^{1/2}$ and bending strength of 404±30 MPa, because the LAS glass has lower TEC than Al_2O_3 and results in compression microstresses at grain boundaries.
3. Strengthening or toughening in alumina ceramics can be achieved by adding glass-phases with suitable TEC, higher and lower TEC than alumina resulting in high toughness and high strength polycrystals, respectively.

References

1. Kingery, W. D., Bowen, H. K. and Uhlmann, D. R., *Introduction to Ceramics*, 2nd edn. Wiley-Interscience, New York, 1976.
2. Watanabe, T., The importance of grain boundary character distribution to grain boundary design and control in ceramics. In *Materials Processing and Design: Grain-Boundary-Controlled Properties of Fine Ceramics II*, *Ceramic Transactions,* Vol. 44, ed. K. Niihara, K. Ishizaki and M. Isotani. 1994 pp.123–134.
3. Guo, J. K. and Ma, L. T., Study on the interface and interphase of ceramics. *5th International Symposium on Ceramic Materials and Components for Engines*, ed. D. S. Yan, X. R. Fu and S. X. Shi. China, 1994, pp.477-482.
4. Watanabe, T., Grain boundary design and control for high temperature materials. *Mater. Sci. Eng.*, 1993, **A166**, 11–28.
5. Huang, L. P., Xu, Y. R., Ma, L. T. and Fu, X. R, Sintering behavior and some high temperature properties study of silicon nitride ceramics with Y_2O_3 and La_2O_3 additives. *Proc. C-MRS 1990, Inter. Symp.*, ed. M. Y. Kong and K. J. Huang. pp. 203–207.
6. Mandal, H., Chen, Y. B. and Thompson, D. P, α-Sialon ceramics with a crystalline melilite grain-boundary phase. *5th International Symposium on Ceramic Materials and Components for Engines,* ed. D. S. Yan, X. R. Fu and S. X. Shi. 1994, pp. 202–205.
7. Gu, H., Pan, X., Cannon, R. and Ruhle, M., Dopant distribution in grain-boundary films in calcia-doped silicon nitride ceramics. *J. Am. Ceram. Soc.*, 1998, **81**, 3125–3135.
8. Kleebe, H., Pezzotti, G. and Ziegler, G., Microstructure and fracture toughness of Si_3N_4 ceramics: combined roles of grain morphology and secondary phase chemistry. *J. Am. Ceram. Soc.*, 1999, **82**, 1857–1867.
9. Kleebe, H., Bruley, J. and Ruhle, M., HREM and AEM studies of Yb_2O_3-fluxed silicon nitride ceramics with and without CaO addition. *J. Eur. Ceram. Soc.*, 1994, **14**, 1–11.
10. Pan, X., Gu, H., Weeren, R., Danforth, S., Cannon, R. and Ruhle, M., Grain-boundary microstructure and chemistry of a hot isostatically pressed high-purity silicon nitride. *J. Am. Ceram. Soc.*, 1996, **79**, 2313–2320.
11. Guo, J. K. and Zhu, P. N., Design of ceramic matrix composite. *Proc. of Inter. Conf. on High Temperature Ceramic Matrix Composites*, ed. R. Naslain, J. Lamon, D. Doumeingts. Woodhead Publishing Limited, France, 1993, pp. 361-368.
12. Chen, I. W. and Xue, L. A., Development of superplastic structural ceramics. *J. Am. Ceram. Soc.*, 1990, **73**, 2585–2609.
13. Jones, R. H., Schilling, C. H. and Schoenlein, L. H., Grain boundary and interfacial chemistry and structure in ceramics and ceramics composites. *Mater. Sci. Forum*, 1989, **46**, 277–308.
14. Watanable, T., Grain boundary design for the control of intergranular fracture. *Mater. Sci. Forum*, 1989, **46**, 25-48.
15. Wiederhorn, S. M., Hockey, B. J., Kranse, R. F. and Jakus, K., Creep and fracture of a vitreous-bonded aluminium oxide. *J. Mater. Sci.*, 1986, **21**, 810–824.
16. Pezzotti, G., Sergo, V., Sbaizero, O., Muraki, N., Meriani, S. and Nishida, T., Strengthening contribution arising from residual stresses in Al_2O_3/ZrO_2 composites: a piezo-spectroscopy investigation. *J. Eur. Ceram. Soc.*, 1999, **19**, 247–253.
17. Pezzotti, G., Nishida, T., Kleebe, H., Ota, K., Muraki, N. and Sergo, V., Effect of interface chemistry on the mechanical properties of Si_3N_4-matrix composites. *J. Mater. Sci.*, 1999, **34**, 1667–1680.
18. Pezzotti, G., Kleebe, H., Ota, K. and Yabuta, K., Suppression of viscous grain-boundary sliding in a dilute SIALON ceramic. *J. Am. Ceram. Soc.*, 1997, **80**, 2349–2354.
19. Shi, J. L., Lu, Z. L. and Guo, J. K., Model analysis of boundary residual stress and its effect on toughness in thin boundary layered yttria-stabilized tetragonal zirconia polycrystalline ceramics. *J. Mater. Res.*, 2000, **15**, 727–732.
20. Powell-Dogan, C. A. and Heuer, A. H., Misconstruction of 96% alumina ceramics: crystallization of high magnesia boundary glasses. *J. Am. Ceram. Soc.*, 1990, **73**, 3677–3683.
21. Travitzky, N. A., Brandon, D. G. and Gutmanas, E. Y., Effect of rapid cooling on the microstructure and mechanical properties of commercial 85 wt.% Al_2O_3. *Mater. Sci. and Eng.*, 1985, **71**, 77–86.
22. Powell-Dogan, C. A., Heuer, A. H., Ready, M. J. and Merriam, K., Residual-stress-induced grain pullout in a 96% alumina. *J. Am. Ceram. Soc.*, 1991, **74**, 646–649.
23. Bennison, S. J. and Lawn, B. R., Role of interfacial grain-bridging sliding friction in the crack-resistance and strength properties of nontransforming ceramics. *Acta Metall.*, 1989, **37**, 2659–2671.
24. Bennison, S. J., Chan, H. M. and Lawn, B. R., Effect of heat

treatment on crack-resistance curves in a liquid-phase-sintered alumina. *J. Am. Ceram. Soc.*, 1989, **72**, 677–679.
25. Dunnell, H. L., Ready, M. J. and Kovar, D., Effect of glass additions on the indentation-strength behavior of alumina. *J. Am. Ceram. Soc.*, 1995, **78**, 849–856.
26. Padture, N. P. and Chan, H. M., Improved flaw tolerance in alumina containing 1 vol.% anorthite via crystallization of the intergranular glass. *J. Am. Ceram. Soc.*, 1992, **75**, 1870–1875.
27. Chen, N. W., Krutyholowa, M. W., Haun, M. J., Brog, T. K., Wirth, D. G., Sibold, J. D. and McNerney,K. R., Crystallization behavior of $BaO–Al_2O_3–SiO_2$ intergranular glass compositions on alumina ceramics. Advance in ceramic–matrix composites. *Ceramic Transactions*, 1993, **38**, 825–835.
28. Powell-Dogan, C. A. and Heuer, A. H., Microstructure of 96% alumina ceramics: crystallization of high-calcia boundary glasses. *J. Am. Ceram. Soc.*, 1990, **73**, 3684–3691.
29. Peterson, I. and Tien, T. Y., Effect of the grain boundary thermal expansion coefficient on the fracture toughness in silicon nitride. *J Am. Ceram. Soc.*, 1995, **78**, 2345–2352.
30. Cai, H., Padture, N. P., Hooks, B. M. and Lawn, B. R., Flaw tolerance and toughness curves in two-phase particulate composites: SiC/glass system. *J. Eur. Ceram. Soc.*, 1994, **13**, 149–157.
31. Anstis, G. R., Chantikul, P., Lawn, B. R. and Marshall, D. B., A critical evaluation of indentation techniques for measuring fracture toughness: Direct crack measurement. *J. Am. Ceram. Soc.*, 1981, **64**, 533–538.
32. Hormadaly, J., Empirical methods for estimating the linear coefficient of expansion of oxide glasses from their composition. *Journal of Non-Cryst. Solids*, 1986, **79**, 311–324.
33. Corral, J. S. and Verduch, A., The solid solution of silica in celsia. *Trans. Br. Ceram. Soc.*, 1978, **77**, 40–44.